Quantum phases of a weakly disordered Josephson ladder

Eyal Walach and Efrat Shimshoni
Department of Physics, Jack and Pearl Resnick Institute and the Institute of Nanotechnology and Advanced Materials, Bar-Ilan University, Ramat-Gan 52900, Israel

(Received 29 March 2021; accepted 18 May 2021; published 1 June 2021)

The interplay of interactions and disorder in low-dimensional superconductors supports the formation of multiple quantum phases as possible instabilities of the superconductor-insulator transition (SIT) at a singular quantum critical point. We explore a one-dimensional model which exhibits such a variety of phases in the strongly quantum fluctuations regime. Specifically, we study the effect of weak disorder on a two-leg Josephson ladder with comparable Josephson and charging energies ($E_J \sim E_C$). An additional key feature of our model is the requirement of perfect $\mathbb{Z}_2$ symmetry, respected by all parameters including the disorder. Using a perturbative renormalization-group (RG) analysis, we derive the phase diagram and identify at least one intermediate phase between a full-fledged superconductor and a disorder-dominated insulator. Most prominently, for repulsive interactions on the rungs we identify two distinct mixed phases: In both of them the longitudinal charge mode is a gapless superconductor, however one phase exhibits a dipolar charge density order on the rungs, while the other is disordered. This latter phase is characterized by coexisting superconducting (phase-locked) and charge-ordered rungs, and encompasses the potential of evolving into a Griffith's phase characteristic of the random-field Ising model in the strong disorder limit.

DOI: 10.1103/PhysRevB.103.245301

I. INTRODUCTION AND PRINCIPAL RESULTS

The superconductor-insulator transition (SIT) observed in thin layers or wires of superconducting (SC) materials is a dramatic manifestation of quantum fluctuations enhanced by the low dimensionality [1–3]. Its most prominent signature is a drastic change in the electric resistance at low temperatures $T \to 0$, which switches from zero to infinity upon tuning of a nonthermal parameter (e.g., a magnetic field, a reduced layer thickness, gating, etc.) beyond a critical value. This phenomenon exemplifies a quantum phase transition (QPT) [4]: a fundamental change in the nature of the ground state across a $T = 0$ critical point.

The onset of a SIT does not necessarily involve the breaking of Cooper pairs: It has been seen in Josephson arrays, granular systems, and disordered metals where superconductivity persists locally even in the insulating phase. In such systems, the underlying mechanism is rather dominated by the combined effects of repulsive interactions and disorder, which tend to impede long-range phase coherence between SC islands in favor of a charge-localized phase. This mechanism is well captured by interacting Bosons models or equivalently Josephson arrays [1,5–12]. In the latter, the competition between a repulsive interaction and the superconducting stiffness is tunable by the ratio of two energy scales—the charging energy E_c and Josephson energy E_J. The SIT occurs at a critical value where $E_c/E_J \sim 1$, corresponding to maximal phase-charge uncertainty.

Disorder is an additional ingredient, associated with the presence of random charge impurities and/or spatial fluctuations in E_c/E_J. Its interplay with the interactions may introduce a richer set of quantum phases, separated by more than one critical point. Indeed, extensive studies have suggested a variety of distinct insulating phases including, e.g., a "Bose/Mott glass" [5,6]. A more intriguing possibility is the emergence of an intermediate metallic phase [13–16] near the putative SIT critical point. Alternatively, a mixed phase with coexisting SC and charge density correlations may form in this strongly fluctuating regime.

In the present paper, we show that several mixed phases are supported in a relatively simple model for a strongly fluctuating SC device. We consider a weakly-disordered two-legged Josephson ladder, focusing on the quantum fluctuations regime where both intra- and interleg charge interactions are comparable to the Josephson coupling on the same links ($E_c \sim E_J$). A crucial property of our model is a perfect $\mathbb{Z}_2$ symmetry, respected by all parameters including the disorder; notably, this is easier to achieve when the leg index represents a discrete degree of freedom other than real-space separation. Contrary to earlier studies of bosonic ladders [17–20], a natural description of the system under these conditions involves a weak coupling between fermionic and bosonic sectors. Utilizing a perturbative renormalization-group (RG) analysis to explore the $T = 0$ phase diagram, we find evidence for a variety of intermediate phases between a full-fledged superconductor and a disorder-dominated insulator (see Fig. 1). Most prominently, we identify two distinct mixed phases where SC correlations coexist with charge ordering: One exhibits long-range CDW order, and one (marked Dis I in the figure) is disordered. We conjecture that in the strong disorder limit, this latter phase evolves into a Griffith's phase characteristic of the random-field Ising model [21].

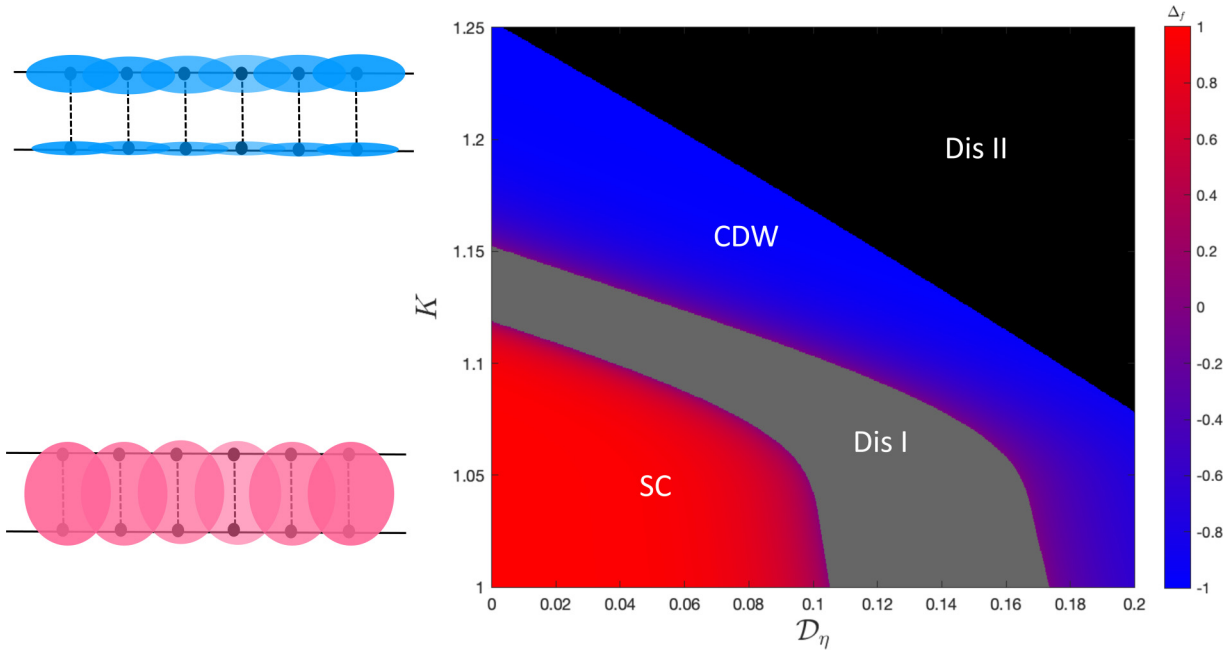

FIG. 1. Left panel: Illustration of the charge configuration on the ladder in the ordered phases; the top panel depicts the CDW-ordered phase and the bottom panel the SC phase. Right panel: Phase diagram as a function of the Luttinger parameter $K = \sqrt{K_+ K_-}$ and disorder $\mathcal{D}_\eta$, for $V > 0$ (see text); here $K_+/K_- = 1.02$, $u_+ = u_- = 1$, $\mathcal{D}_{g,-} = 0.003$, $g_\theta = 0.3$, $g_\phi = 0.03$, $\mathcal{D}_{U,s} = 0$; the color scale denotes $\Delta(\ell_f)$ obtained from the RG flow up to $\ell_f = 20$. The gray region (Dis I) corresponds to the intermediate disordered phase where $\mathcal{D}_-$ is relevant, but the symmetric mode maintains a LL behavior; the black region (Dis II) corresponds to the disordered insulator where $\mathcal{D}_g$ is relevant.

A key feature of the bosonic ladder in the clean limit is the separability of the low-energy degrees of freedom into two independent sectors: the symmetric (longitudinal) and antisymmetric (transverse) modes. Each of the sectors may undergo a QPT of distinct type, associated with the breaking of $U(1)$ and $\mathbb{Z}_2$ symmetries, respectively. In the quantum fluctuations regime, the antisymmetric mode (best represented in terms of nearly-free fermions) exhibits an Ising-type QPT [22,23]. Under the extra assumption of commensurate boson density on the lattice, the symmetric mode exhibits a Berezinskii-Kosterlitz-Thouless (BKT) transition [24,25] from a Luttinger liquid (LL) to a Mott insulator. Consequently, as a common parameter is tuned (e.g., E_c/E_J on the legs), an intermediate phase can emerge between the two separate critical points, with coexisting charge density wave (CDW) order of the global charge and a SC order with interleg phase locking.

What is the fate of this intermediate phase in the presence of disorder? One possible scenario is the shrinking of this phase and recovery of a singular SIT critical point. On the other hand, disorder supports the formation of inhomogeneity and thus stabilizes the coexistence of spatially separate regions with distinct local order parameters [26]. Specifically in our case, two different types of disorder effects should be considered. The first type, resulting mainly from inhomogeneities in the charging and Josephson energies, maintains the fermionic and bosonic sectors independently, but possibly alters the nature and position of the respective critical points. The other type of disorder may introduce coupling terms between the two sectors which may profoundly change the critical behavior of the combined boson-fermion system, e.g., turning the continuous Ising transition into first order or generating a novel multicritical point [27–29]. A dominant effect of the latter type stems from the presence of random impurities which induce spatial fluctuations in the chemical potential along the ladder. As detailed below, we analyze the interplay between both types of disorder and derive their combined effect on the phase diagram.

The rest of this paper is organized as follows: In Sec. II we introduce the model; in Sec. III we present the RG analysis and main results; our concluding remarks are summarized in Sec. IV. Finally, Appendices A through D are devoted to technical details of our analysis.

II. THE MODEL

As a starting point, we consider the clean limit of a two-leg bosonic ladder described by the Hamiltonian

$$H_0 = \int dx[\mathcal{H}_1 + \mathcal{H}_2 + \mathcal{H}_{\text{int}}], \tag{1}$$

where x is a continuous coordinate along the leg direction (in units of the lattice constant a), and the local terms are given by

$$\mathcal{H}_\nu = \tfrac{1}{2}\left[U\rho_\nu^2 + \rho_s(\partial_x\phi_\nu)^2\right] \ (\nu = 1, 2) \tag{2}$$

$$\mathcal{H}_{\text{int}} = [-J\cos(\phi_1 - \phi_2) + V\rho_1\rho_2]. \tag{3}$$

Here U is the charge interaction and ρ_s the superfluid stiffness within each leg, J is the interleg Josephson coupling and V is the interleg charge interaction; $\rho_\nu(x)$, $\phi_\nu(x)$ are, respectively, the local charge-density fluctuation and phase operators on leg

ν. We further use the expansion [30]

$$\rho_\nu = -\frac{1}{\pi}\partial_x\theta_\nu + \rho_0 \sum_{p\in\mathbb{Z}\setminus 0} e^{i\cdot 2p\cdot(\theta_\nu - \pi\rho_0 x)}, \tag{4}$$

where $\partial_x\theta_\nu$ and ϕ_ν are canonical conjugates, and ρ_0 denotes the uniform background charge density.

Since H_0 obeys a $\mathbb{Z}_2$ symmetry to exchange between the legs, its low-energy approximation can be decomposed into independent symmetric (+) and antisymmetric (−) sectors using the transformation

$$\theta_\pm = \frac{\theta_1 \pm \theta_2}{\sqrt{2}}, \quad \phi_\pm = \frac{\phi_1 \pm \phi_2}{\sqrt{2}}. \tag{5}$$

Accounting for the leading terms in Eq. (4) (see Appendix A for details), this yields $H_0 = H_+ + H_-$ where each subsystem independently exhibits a QPT tunable by a common parameter of H_0, e.g., $K \propto \sqrt{\frac{U}{\rho_s}}$.

The symmetric part H_+ is a sine-Gordon (SG) model:

$$H_+ = \int dx[\mathcal{H}_{LL}^{(+)} + g\cos(\sqrt{8}\theta_+ - 2\pi\rho_0 x)],$$
$$\mathcal{H}_{LL}^{(+)} = \frac{u_+}{2\pi}\left(K_+(\partial_x\theta_+)^2 + \frac{1}{K_+}(\partial_x\phi_+)^2\right) \tag{6}$$

which exhibits a Luttinger liquid (LL) behavior corresponding to a gapless plasmon mode for generic values of ρ_0. However close to integer filling of the underlying lattice, a transition to a Mott insulator occurs when the Luttinger parameter $K_+ \sim \sqrt{\frac{(U+V)}{\rho_s}}$ exceeds a critical value; this is a SIT where the SC phase exhibits only a quasi-long-range order.

In contrast, H_- describing the antisymmetric mode is a self-dual SG model (SDSG) [31]

$$H_- = \int dx[\mathcal{H}_{LL}^{(-)} - g_\phi\cos\sqrt{2}\phi_- + g_\theta\cos\sqrt{8}\theta_-],$$
$$\mathcal{H}_{LL}^{(-)} = \frac{u_-}{2\pi}\left(K_-(\partial_x\theta_-)^2 + \frac{1}{K_-}(\partial_x\phi_-)^2\right) \tag{7}$$

in which the competing phase-locking and charge-locking cosine terms arise from the corresponding two terms of Eq. (3). In a wide range of parameters surrounding the self-duality point $K_- = 2$, $g_\phi = g_\theta$ [accessible for $U \sim \rho_s$ in Eq. (2) and $J \sim V\rho_0^2$], both of them are simultaneously relevant and the SDSG is effectively described as two independent transverse-field Ising models, one of which is highly massive [23,32]. The low-energy description is therefore given in terms of a single pair of Majorana fields ξ_R, ξ_L:

$$H_- = \int dx(\xi_R(-iu_-\partial_x)\xi_R - \xi_L(-iu_-\partial_x)\xi_L - i\Delta\xi_R\xi_L) \tag{8}$$

which indicates an Ising-type transition when the gap Δ changes sign. This can be interpreted as a SIT as well: the $\Delta > 0$ phase [realized when J in Eq. (3) is sufficiently larger than $V\rho_0^2$] is phase locked (i.e., SC), while $\Delta < 0$ (corresponding to the opposite case) is a Mott insulator; both phases are long-range ordered (with a gap $|\Delta|$). Note that the nature of CDW order in the insulator depends on the sign of V: For $V > 0$, dipoles are formed on the rungs ($\theta_- = \pm\pi/\sqrt{8}$), while $V < 0$ favors equal charges on the two legs ($\theta_- = 0$).

We now introduce disorder resulting from random x-dependent variations in the various parameters of the model. We distinguish two types of disorder, as detailed below.

(a) *Particle-hole preserving disorder.* We first consider randomness arising from spatial inhomogeneities in the parameters U, ρ_s, J, and V of the original model Eqs. (2) and (3) related to the charging and Josephson energies on the legs and rungs of the ladder. Such corrections to the Hamiltonian do not couple linearly to the density operators and hence do not violate particle-hole symmetry when the chemical potential adjusts ρ_0 to a commensurate filling. At the same time this type of disorder maintains the $\mathbb{Z}_2$ symmetry of the model; hence it does not couple the symmetric and antisymmetric sectors and is ultimately manifested as randomness in the parameters of H_+, H_- [Eqs. (6) and (8)]. Notably, since the disorder is space dependent but not time dependent, it breaks the Lorentz symmetry characterizing both low-energy degrees of freedom; hence (as we show explicitly in the next section) all the parameters including the velocities $u_\pm$ flow under RG.

The disorder in the symmetric sector is introduced as x-dependent corrections to the parameters K_+, u_+, and g; all of these can be assumed to originate from a term $\delta\mathcal{H}_\nu(x)$ of the form Eq. (2) with random charging energy $\delta U(x)$ and superfluid stiffness $\delta\rho_s(x)$. We further assume that these random corrections are the same on both legs $\nu = 1, 2$ and correspond to a static "white noise" characterized by the disorder averages

$$\langle\langle\delta U(x)\rangle\rangle = 0, \quad \langle\langle\delta\rho_s(x)\rangle\rangle = 0$$
$$\langle\langle\delta U(x)\delta U(x')\rangle\rangle = D_U\delta(x-x') \tag{9}$$
$$\langle\langle\delta\rho_s(x)\delta\rho_s(x')\rangle\rangle = D_s\delta(x-x').$$

As shown in the next section, these disorder terms renormalize the parameters K_+, u_+ of the quadratic part $\mathcal{H}_{LL}^{(+)}$ in Eq. (6) but are irrelevant under RG. More significant is their effect on the cosine term, which we maintain as an independent disorder term associated with random corrections to g:

$$H_g = \frac{1}{2}\int dx(\delta g(x)e^{i\sqrt{8}\theta_+} + \delta g^*(x)e^{-i\sqrt{8}\theta_+}), \tag{10}$$

where the complex parameter $\delta g(x)$ contains the oscillatory phase shift of θ_+ and is characterized by the disorder averages

$$\langle\langle\delta g(x)\delta g(x')\rangle\rangle = \langle\langle\delta g(x)\rangle\rangle = 0,$$
$$\langle\langle\delta g(x)\delta g^*(x')\rangle\rangle = D_g\delta(x-x'). \tag{11}$$

In the antisymmetric sector, the disorder characterized by D_U, D_s [Eq. (9)] combined with random fluctuations in the rung interactions J, V generate x dependence in all the parameters of Eq. (7). However, within the regime of parameters where the low-energy theory for H_- is captured by Eq. (8), we encode their most prominent contribution in a single additional disorder parameter corresponding to spatially dependent corrections to the mass Δ:

$$\langle\langle\delta\Delta(x)\rangle\rangle = 0,$$
$$\langle\langle\delta\Delta(x)\delta\Delta(x')\rangle\rangle = D_-\delta(x-x'). \tag{12}$$

Mapping to the Ising model, $\delta\Delta(x)$ can be interpreted as a random transverse field.

(b) *Disordered chemical potential.* We next consider randomness in the chemical potential, arising, e.g., due to

charged impurities in the system. However, to maintain the $\mathbb{Z}_2$ symmetry we assume the local potential $\delta\mu(x)$ to be identical on the two legs. The leading term added to H_0 of Eq. (1) is of the form

$$H_\eta = \frac{1}{2}\sum_\nu \int dx(\eta(x)e^{i2\theta_\nu} + \eta^*(x)e^{-i2\theta_\nu}) = \int dx(\eta(x)e^{i\sqrt{2}\theta_+} + \eta^*(x)e^{-i\sqrt{2}\theta_+})\cos\sqrt{2}\theta_-, \quad (13)$$

where $\eta(x)$ is a complex random variable obeying

$$\langle\langle \eta(x)\eta(x')\rangle\rangle = \langle\langle \eta(x)\rangle\rangle = 0, \quad \langle\langle \eta(x)\eta^*(x')\rangle\rangle = D_\eta\delta(x-x'). \quad (14)$$

Distinctly from all the previous disorder terms, this introduces a nontrivial coupling term between the symmetric and antisymmetric sectors of H_0. In terms of their low-energy degrees of freedom, it corresponds to a many-body boson-fermion interaction, which in particular does not have a simple local form in terms of the fermion fields of Eq. (8).

Accounting for all types of disorder introduced in (a) and (b) as weak perturbations of H_0, we next derive RG equations in the spirit of the analysis described, e.g., in Ref. [33] (see Appendix B for details). It is noteworthy that the special case $D_\eta = 0$, which allows treatment of the $\pm$ sectors independently, indeed reduces the problem to models studied elsewhere in the literature. However, the more generic case where D_η is finite yields a set of coupled RG equations which affects all parameters of the model and in particular generates all other types of disorder (most prominently, D_g and D_-) even when their bare values are zero. Below we sketch the main steps and results of this RG analysis.

III. RG ANALYSIS AND MAIN RESULTS

The various disorder terms described in the previous section affect the behavior of the system in different ways. We use a perturbative momentum-shell RG method (see Appendix B for details) in order to determine their effect on the system, which will allow us to explore the different parts of the phase diagram. We shall begin with the case $D_\eta = 0$ and analyze the disorder terms of type (a), which affect each of the $\pm$ sectors independently (Secs. III A and III B below); in Sec. III C we introduce $D_\eta \neq 0$ which couples the two sectors and yields the full phase diagram.

A. Symmetric sector

First, we consider the symmetric sector H_+. The clean part is described by Eq. (6), to which we add three types of disorder: D_U, D_s [Eq. (9)] and D_g [Eq. (10)]. The full Hamiltonian for the symmetric sector acquires the form

$$H_+ = \int dx[\mathcal{H}_{LL}^{(+)} + \delta U(x)(\partial_x\theta_+)^2 \quad (15)$$

$$+ \delta\rho_s(x)(\partial_x\phi_+)^2 + [\delta g(x)e^{i\sqrt{8}\theta_+} + \text{H.c.}]]\ ; \quad (16)$$

note that here we assume a generic filling for which the oscillatory cosine term in Eq. (6) can be eliminated. The quadratic disorder parameters are better written in a dimensionless form:

$$\mathcal{D}_{U/s} = \frac{D_{U/s}\Lambda}{(2\pi)^4 u_+^2}, \quad (17)$$

where Λ is the upper momentum cutoff. Along with the definition from Ref. [33],

$$\mathcal{D}_g = \frac{D_g}{\Lambda^3 u_+^2}, \quad (18)$$

one can write the RG equations for the symmetric sector:

$$\begin{aligned}
\frac{dK_+}{d\ell} &= 4\left(\mathcal{D}_s K_+^2 + \frac{\mathcal{D}_g}{K_+} - \frac{\mathcal{D}_U}{K_+^2}\right)K_+ \\
\frac{du_+}{d\ell} &= -4\left(\mathcal{D}_s K_+^2 + \frac{\mathcal{D}_g}{K_+} + \frac{\mathcal{D}_U}{K_+^2}\right)u_+ \\
\frac{d\mathcal{D}_{s/U}}{d\ell} &= -\mathcal{D}_{s/U} \\
\frac{d\mathcal{D}_g}{d\ell} &= \left(3 - \frac{4}{K_+}\right)\mathcal{D}_g,
\end{aligned} \quad (19)$$

where ℓ is the logarithmic rescaling factor. One readily observes that the disorder in the quadratic terms ($\mathcal{D}_{s/U}$) is always irrelevant, and so it just renormalizes the parameters K_+ and u_+ (see Appendix C 1). The Luttinger parameter K_+ can be renormalized either upwards or downwards, while the velocity is always corrected downwards—this results from breaking the Lorenz invariance of the system. As these disorder terms only contribute corrections to the parameters of the clean model and are never relevant, in the forthcoming more complex analysis we will ignore them and just use the effective values of K_+, u_+.

On the contrary, $\mathcal{D}_g$ turns relevant at $K_c = \frac{4}{3}$. This critical value might be modified due to $D_{s/U}$, but the general structure is the same. The exact value depends on the parameters, but around $K_+ = K_c$ one can find a critical manifold where the symmetric sector undergoes a SIT. The superconducting phase is a LL with power-law correlations which manifests zero resistance only in the limit $T \to 0$, and the insulating phase is a disordered insulator, dominated by D_g.

B. Antisymmetric sector

Next, we turn to the antisymmetric sector H_-. The clean part of the Hamiltonian is given most generally by Eq. (7). One should note that for very low values of K_- ($K_- < 1$), the term $g_\theta\cos\sqrt{8}\theta_-$ turns irrelevant and the CDW order it tends to induce is completely suppressed. In that case, the system will be a gapped superconductor, where the relative phase ϕ_- is locked by the Josephson coupling. Similarly, for high values of K_- ($K_- > 4$), the system is a gapped insulator with CDW order parameter.

For values of K_- in the intermediate regime between these two extremes the system is well described by the fermionic Hamiltonian Eq. (8), on which we focus. Apart from the disorder terms $D_{s/U}$, whose effects we will include in the definitions of u_- and K_-, here the dominant disorder will be in the gap parameter Δ, i.e., D_- defined in Eq. (12). This disorder can be treated similarly to D_g, but as D_- is always relevant we account for second order contributions to get

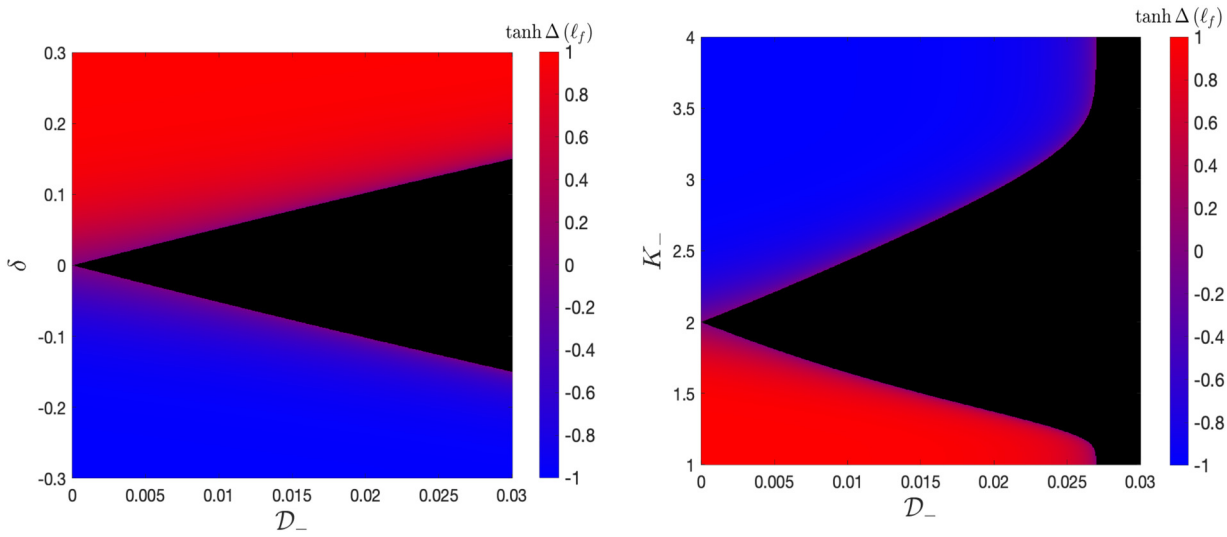

FIG. 2. Left panel: Phase diagram of the antisymmetric sector for $D_\eta = 0$, as a function of the gap Δ and disorder in the gap $\mathcal{D}_-$. Here $u_- = 1$; the color code denotes $\Delta(\ell_f)$ obtained from the RG flow up to $\ell_f = 10$. The black region corresponds to the disordered phase where the perturbative analysis breaks down. Right panel: the same phase diagram, parametrized by the Luttinger parameter of the antisymmetric sector K_-; the dependence of the gap on K_- is monotonic but nonlinear, taken from Ref. [23]. In both panels, red is superconductor and blue is insulator.

a more accurate description of the behavior. We define the dimensionless disorder parameter

$$\mathcal{D}_- = \frac{D_-}{(2\pi)^2 u_-^2 \Lambda}; \tag{20}$$

along with the normalized gap $\delta \equiv \frac{\Delta}{u_- \Lambda}$ one can write the equations:

$$\begin{aligned} \frac{d\mathcal{D}_-}{d\ell} &= \mathcal{D}_- + \frac{4}{3}\frac{\delta^2}{(1+\delta^2)^2}\mathcal{D}_-^2 \\ \frac{du_-}{d\ell} &= -\frac{\mathcal{D}_-}{1+\delta^2}u_- \\ \frac{d\delta}{d\ell} &= \left(1 - \frac{2\mathcal{D}_-}{1+\delta^2}\right)\delta. \end{aligned} \tag{21}$$

The above form hints towards a normalized disorder parameter, which accounts better for the simultaneous growth of δ: $\tilde{\mathcal{D}}_- \equiv \frac{\mathcal{D}_-}{1+\delta^2}$, that obeys the equation

$$\frac{d\tilde{\mathcal{D}}_-}{d\ell} = \tilde{\mathcal{D}}_- \frac{1 - \left(1 - \frac{16}{3}\tilde{\mathcal{D}}_-\right)\delta^2}{1+\delta^2}. \tag{22}$$

This yields a threshold value $\tilde{\mathcal{D}_-} = \frac{3}{16}$ below which the disorder $\tilde{\mathcal{D}}_-$ is less relevant than δ, and the system in dominated by the clean limit (see further discussion in Sec. III C 2).

The resulting phase diagram is depicted in Fig. 2. For low enough initial Δ, $\mathcal{D}_-$ one finds that the disorder dominates in a triangle in parameter space, $|\delta| \leqslant \alpha\mathcal{D}_-$ with some constant α. Higher initial values of $\mathcal{D}_-$ introduce nonlinearity in the behavior, but the qualitative behavior is the same—phase-locked superconductor for large positive Δ (low K_-), disorder for small Δ (intermediate K_-), and charge-locked insulator for large negative Δ (high K_-).

The primary conclusion is that here, the SIT occurs via an intermediate phase characterized by a wide distribution of the gap parameter Δ, with tails in either signs. While a full characterization of its behavior requires a nonperturbative method, we interpret this phase as a Bose glass which exhibits local CDW or SC order in random locations in space (and likely develops to a Griffith's phase in the strong disorder limit). Interestingly, this $T = 0$ phase diagram resembles the finite T characteristic of a clean Ising transition in 1+1 dimensions, with $\mathcal{D}_-$ providing the analog of temperature; a direct transition from CDW to SC occurs only at the singular QCP $\mathcal{D}_- = \Delta = 0$.

C. Disordered coupling term

We next analyze the disorder term H_η [Eq. (13)], which couples the $\pm$ sectors. As a basis for a perturbative RG analysis of this term, we assume $D_\eta \ll u_\pm^2 \Lambda^3$ and take advantage of the known correlations of the operators $\cos\sqrt{2}\theta_-$, $e^{\pm i\sqrt{2}\theta_+}$ in their respective independent unperturbed states dictated by $H_\pm$ [Eqs. (6) and (7)]. Notably, the former operator controlling the coupling to the antisymmetric mode does not have a simple representation in terms of the Fermions characterizing the low-energy degrees of freedom for intermediate values of K_- [Eq. (8)]. However, its space-time correlations are well characterized in terms of the order and disorder Ising fields [32] and are crucially dependent on the sign of Δ. In particular, for $\Delta > 0$ where the antisymmetric sector is in the SC phase, its correlations are exponentially decaying.

In the insulating phase of H_- established for $\Delta < 0$, the disorder term H_η couples to a more relevant operator compared to the SC phase. However, its ultimate effect on the behavior of the system depends on an additional ingredient of the model: the *sign* of the interleg interactions V [see Eq. (3)] or equivalently the coefficient g_θ in Eq. (7). As noted

in Sec. II, in the clean limit this determines the charge ordering pattern on the rungs: For repulsive interactions ($V > 0$), the charge field is locked at either one of the minima $\theta_- = \pm\pi/\sqrt{8}$ for which $\langle\cos\sqrt{2}\theta_-\rangle = 0$; in the case of attractive interactions ($V < 0$), $\theta_- = 0, \pi/\sqrt{2}$ yielding $\langle\cos\sqrt{2}\theta_-\rangle \neq 0$, and hence H_η couples to the total-charge mode via a highly relevant operator $\cos\sqrt{2}\theta_+$. We therefore separate these two cases in our analysis.

We first consider the repulsive interaction case $V > 0$, which turns out to yield a richer phase diagram. In this case, $\cos\sqrt{2}\theta_-$ has no expectation value, and its correlators decay exponentially. As a result, the only contribution of H_η to the RG equations to leading (linear) order in D_η will be manifested as shifts of the parameters g, g_θ in the clean model. The leading nontrivial contribution beyond that arises from fourth order in the perturbation expansion; it can be interpreted as a quenched disorder term of a higher scaling dimension compared to all types of terms introduced in Sec. II and is irrelevant in all the ordered phases of the $D_\eta = 0$ case (see Appendix B for details). Consequently, the latter effect of a finite D_η on the RG equations can be neglected.

To set up the derivation of RG equations at finite D_η, we first define the dimensionless disorder parameter

$$\mathcal{D}_\eta \equiv \frac{D_\eta}{u^2\Lambda^3}; \tag{23}$$

here a velocity scale $u \approx \min\{u_+, u_-\}$ is introduced, noting that D_η couples to both sectors. As discussed above, the effect of $\mathcal{D}_\eta$ on the RG flow strongly depends on the behavior of the antisymmetric mode in the clean limit. We therefore consider below three limits, classified most conveniently by the (bare) value of the parameter K_-: the bosonic superconductor, the bosonic insulator, and the intermediate fermionic regime.

1. Bosonic superconductor ($K_- < 1$)

This regime is established when the last term in Eq. (7) is irrelevant, and H_- reduces to a standard sine-Gordon model dominated by the single cosine term describing Josephson coupling on the rungs. The antisymmetric mode is then in a gapped phase where the relative phase field ϕ_- is locked at $\phi_- = 0$; low-energy quantum fluctuations in ϕ_- are well described by a massive bosonic model. We note that this behavior is not significantly altered even if randomness in the mass is introduced (see Appendix D). As already noted, in this case any operator of the form $\cos\gamma\theta_-$ coupling to the dual field is exponentially irrelevant. As a result, the sole effect of $\mathcal{D}_\eta$ is to provide corrections to the other parameters of the model which can be absorbed in their bare values and hence practically ignored.

2. Bosonic insulator ($K_- > 4$)

In this regime of parameters, the last term in Eq. (7) is dominant while the Josephson coupling on the rungs turns irrelevant. As a result, one obtains a strong tendency for charge locking in the antisymmetric sector at a CDW pattern obeying $\langle\cos\sqrt{8}\theta_-\rangle \approx -1$, and H_- can be approximated by a massive bosonic model with gap $|\Delta|$ (in terms of the definitions of Sec. II, $\Delta < 0$). However, since at the same time $\langle\cos\sqrt{2}\theta_-\rangle \approx 0$, the leading contribution to the RG equation for the disorder term arises from order D_η^2 (see Appexdix B). The linear order in $\mathcal{D}_\eta$, on the other hand, generates terms which can be regarded as corrections to the various parameters of H_0. Combining them all, we get the following set of coupled equations:

$$\begin{aligned}
\frac{dK_+}{d\ell} &= 4\left(\mathcal{D}_s K_+^2 + \frac{2\mathcal{D}_g}{K_+} - \frac{\mathcal{D}_U}{K_+^2}\right)K_+ + \left(\frac{u_+}{u}\right)\mathcal{D}_\eta \\
\frac{du_+}{d\ell} &= -4\left(\mathcal{D}_s K_+^2 + \frac{2\mathcal{D}_g}{u_+} + \frac{\mathcal{D}_U}{K_+^2}\right)u_+ - \left(\frac{u_+}{u}\right)\frac{u_+}{K_+}\mathcal{D}_\eta \\
\frac{dK_-}{d\ell} &= 4\left(\mathcal{D}_s K_-^2 - \frac{\mathcal{D}_U}{K_-^2}\right)\frac{K_-}{1+\delta^2} + \left(\frac{u_-}{u}\right)\mathcal{D}_\eta \\
\frac{du_-}{d\ell} &= -4\left(\mathcal{D}_s K_-^2 + \frac{\mathcal{D}_U}{K_-^2}\right)\frac{u_-}{1+\delta^2} - \left(\frac{u_-}{u}\right)\frac{u_-}{K_-}\mathcal{D}_\eta \\
\frac{d\delta}{d\ell} &= \delta - \delta^{2/K_- - 1}\frac{u_+}{u_-}\mathcal{D}_\eta \\
\frac{d\mathcal{D}_U}{d\ell} &= -\mathcal{D}_U \\
\frac{d\mathcal{D}_s}{d\ell} &= -\mathcal{D}_s \\
\frac{d\mathcal{D}_g}{d\ell} &= \left(3 - \frac{4}{K_+}\right)\mathcal{D}_g + c\mathcal{D}_\eta^2 \\
\frac{d\mathcal{D}_\eta}{d\ell} &= \left(\frac{3}{2} - \frac{2}{K_+} - \frac{2}{K_-(1+\delta^2)}\right)\mathcal{D}_\eta,
\end{aligned} \tag{24}$$

where c is a constant of order unity. It is noteworthy that the two bosonic descriptions mentioned above are valid approximations even when both cosine terms are relevant, if one of them has a significantly larger effect on the system, as quantified by the gaps they induce [23]; see Appendix A.

3. Fermionic regime (intermediate values of K_-)

In this regime where the clean part of the antisymmetric sector is best approximated by the fermionic model Eq. (8), the effect of $\mathcal{D}_\eta$ on the RG equations is similar in nature to the previous case; the primary difference is that the operator $\cos\sqrt{8}\theta_-$ which couples to the leading terms generated by the disorder can be more conveniently expressed in terms of fermion fields. This yields the following set of coupled equations (see Appendix B for details):

$$\begin{aligned}
\frac{dK_+}{d\ell} &= 4\left(\mathcal{D}_s K_+^2 + \frac{2\mathcal{D}_g}{K_+} - \frac{\mathcal{D}_U}{K_+^2}\right)K_+ + \left(\frac{u_+}{u}\right)\mathcal{D}_\eta \\
\frac{du_+}{d\ell} &= -4\left(\mathcal{D}_s K_+^2 + \frac{2\mathcal{D}_g}{K_+} + \frac{\mathcal{D}_U}{K_+^2}\right)u_+ - \left(\frac{u_+}{u}\right)\frac{u_+}{K_+}\mathcal{D}_\eta \\
\frac{du_-}{d\ell} &= -4\left(\mathcal{D}_s K_-^2 + \frac{\mathcal{D}_U}{K_-^2}\right)\frac{u_-}{1+\delta^2} - \left(\frac{u_-}{u}\right)\frac{u_-}{K_-}\mathcal{D}_\eta - \frac{\mathcal{D}_-}{1+\delta^2}u_- \\
\frac{d\delta}{d\ell} &= \delta - C_{g_\theta}\frac{u_+}{u_-}\mathcal{D}_\eta - \frac{2\mathcal{D}_-}{1+\delta^2}\delta \\
\frac{d\mathcal{D}_U}{d\ell} &= -\mathcal{D}_U \\
\frac{d\mathcal{D}_s}{d\ell} &= -\mathcal{D}_s
\end{aligned}$$

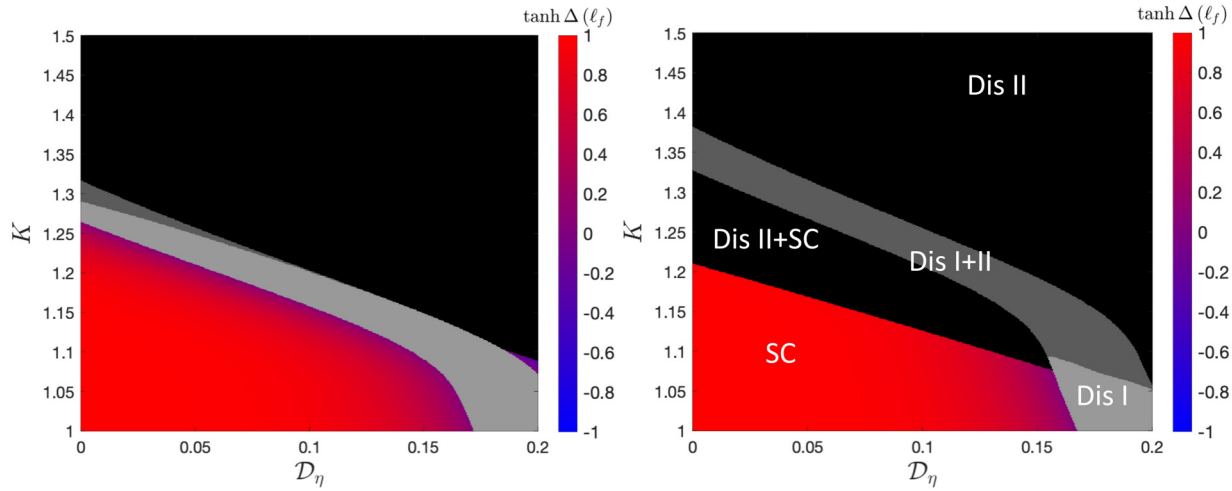

FIG. 3. Phase diagrams as a function of K and $\mathcal{D}_\eta$ for $V > 0$, and different values of the ratio K_+/K_-. In both panels $u_+ = u_- = 1$, $\mathcal{D}_g = \mathcal{D}_- = 0.002$, $g_\theta = 0.2$, $g_\phi = 0.05$, and $\mathcal{D}_{U,s} = 0$. Left: $K_+/K_- = 0.98$; Right: $K_+/K_- = 1.08$. The titles of the phases match the definitions from Fig. 1, Dis I+II is a phase where both disorder terms are relevant, and Dis II+SC is a potential intermediate phase where SC order in the antisymmetric sector coexists with disorder in the symmetric sector.

$$\begin{aligned}
\frac{d\mathcal{D}_g}{d\ell} &= \left(3 - \frac{4}{K_+}\right)\mathcal{D}_g + c_1\mathcal{D}_\eta^2 \\
\frac{d\mathcal{D}_-}{d\ell} &= \mathcal{D}_- + \frac{4}{3}\frac{\delta^2}{(1+\delta^2)^2}\mathcal{D}_-^2 + c_2\mathcal{D}_\eta^2 \\
\frac{d\mathcal{D}_\eta}{d\ell} &= \left(\frac{1}{2} - \frac{2}{K_+}\right)\mathcal{D}_\eta.
\end{aligned} \tag{25}$$

Here c_1, c_2 are constants of order unity; $C_{g_\theta} = \left(\frac{16\pi g_\theta}{u_- K_- \Lambda^2}\right)^{\frac{2/K_- - 1}{2-2/K_-}}$ does not change significantly in the regime of parameters where Eq. (25) is valid, so one can consider it as a constant as well.

It is evident from the above two sets of equations that in both cases, $\mathcal{D}_\eta$ turns relevant for high values K_+ which exceed the critical point ($K_+ = \frac{4}{3}$) for $\mathcal{D}_g$ to become relevant. Beyond this critical point which indicates a localization transition in the symmetric sector, the perturbative analysis breaks down, leading to a rapid growth of K_+ and consequently of $\mathcal{D}_\eta$. We therefore conclude that there is effectively a unique disordered insulating phase. Within the framework of the weak-disorder approximation, it is not possible to infer the precise nature of the charge-density pattern on the rungs in this phase, though it may survive locally in randomly distributed disconnected domains.

It should be noted, however, that while $\mathcal{D}_\eta$ does not tune a phase-transition separable from the one dominated by $\mathcal{D}_g$, its coupling to both the symmetric and antisymmetric sectors generates a flow of all the other parameters [see Eqs. (24) and (25)]. As a result, it can serve as the tuning parameter for various transitions, as can be seen in Fig. 1. This figure was obtained by setting the bare parameters to the fermionic regime where the RG flow is determined by Eq. (25) and exhibits a pronounced effect of $\mathcal{D}_\eta$. We identify four distinct phases, accessible, e.g., by tuning $\mathcal{D}_\eta$ upwards: For relatively low values of $\mathcal{D}_\eta$ and K, the symmetric mode is a gapless LL while the antisymmetric mode undergoes a transition from a phase-locked SC phase to a CDW-ordered insulator via a disordered intermediate phase, whose nature is described in Sec. III B above; the fourth phase realized beyond a critical line in the $\mathcal{D}_\eta$-K plane is a disordered insulator, characterized primarily by localization of the symmetric charge mode. Since D_η couples the sectors, this will be the case in the antisymmetric sector as well.

Although Fig. 1 captures the richness of the phase diagram for typical parameters, tuning the parameters differently can introduce other phases. Specifically, the tuning parameter $\frac{K_+}{K_-}$ can change the order of the transitions: D_g may turn relevant before D_Δ. Two exemplary figures with different topology of the phase-diagram can be seen in Fig. 3. It is suggestive that a variety of distinct disordered phases are generated (see black regions and different shades of gray in the figure).

Based on the weak-disorder approximation applied in our study, one cannot reliably deduce the exact nature of these phases. However, it appears that within the regime where a disordered insulator is established in the symmetric sector, some of the independent behavior of the antisymmetric sector still persists. In particular, there appears to be a regime where D_Δ is relevant and dominates the antisymmetric sector, denoted by "Dis I+II" in Fig. 3; more interestingly, there is potentially a mixed phase where the antisymmetric sector still exhibits robust superconductivity, denoted "Dis II+SC" in the figure.

We finally consider the crucially different case where the interactions on the rungs of the ladder are attractive, $V < 0$. The most significant effect of this change of sign is manifested in the sign reversal of the parameter g_θ in Eq. (7); it is therefore equivalent to performing a shift $\theta_- \to \theta_- + \frac{\pi}{\sqrt{8}}$ in the last cosine term in H_- while maintaining the other parts of the clean Hamiltonian the same. The resulting effect on the behavior of $\mathcal{D}_\eta$ is dramatic: The CDW pattern in the insulating phase of the antisymmetric sector favors $\theta_- = 0$,

which corresponds to equal charge densities on the two legs of the ladder. In this ground state, the operator $\cos\sqrt{2}\theta_-$ in H_η [Eq. (13)] has a finite expectation value.

As a result, $\mathcal{D}_\eta$ has a much larger contribution and in the charge-locked phase of the antisymmetric mode yields the following RG equation:

$$\frac{d\mathcal{D}_\eta}{d\ell} = \left(3 - \frac{1}{K_+}\right)\mathcal{D}_\eta. \tag{26}$$

This corresponds to a highly relevant disorder, with critical Luttinger parameter of $K_{+c} = \frac{1}{3}$. We conclude that once the antisymmetric sector transitions into the insulating phase (which happens for K_- way above this critical value), $\mathcal{D}_\eta$ turns relevant. Notably, since its effect on the other disorder parameters is similar to what we have obtained in the $V > 0$ case, this induces their divergence and consequently the formation of a disordered insulating phase. The prominent change in the phase diagram as compared to Fig. 1 is that the intermediate phase manifesting CDW order on the rungs will disappear; the sole intermediate phase separating the SC from a disordered insulator will be the mixed phase marked by a gray region in Fig. 1, where randomness in established in the antisymmetric sector while the symmetric mode remains gapless.

IV. DISCUSSION

In this work we have discussed a two-leg ladder model of a strongly fluctuating superconductor in the presence of various types of quenched disorder and examined the resulting $T = 0$ phases. We found that by tuning a parameter K—which is controlled by the ratio of charging and Josephson energies—or the disorder strength, the system typically undergoes a sequence of quantum phase transitions rather than a direct SIT. Between the two extreme phases—a SC phase manifesting robust phase locking on the rungs and a disordered insulator—at least one intermediate phase is formed. Particularly, in the case of repulsive interactions across the rungs, two distinct intermediate phases are identified: one ordered and one disordered. The ordered phase is characterized by a dipolar CDW order on the rungs, while the disordered intermediate phase exhibits Griffith's singularities interpolating between phase and charge locking on the rungs; in both these mixed phases, as well as in the SC phase, the longitudinal plasmon mode (corresponding to fluctuations in the total charge) maintains a gapless LL behavior and perfect conduction ($R \to 0$) is achieved in the limit $T = 0$. At the opposite extreme, a full-fledged localization of this mode occurs only in the disordered insulator phase (see Fig. 1).

The richness of this phase diagram rests on the symmetry between the two legs, which restricts spatial variations in the parameters to the longitudinal direction. This ensures a relative resilience to weak disorder of the separability between antisymmetric (transverse) and symmetric (longitudinal) phase/charge fluctuation modes. As a consequence, in the former sector we observe traces of behavior characteristic to the Ising model in a random transverse field [21]. Most prominently, in the case where the interleg charge interaction is repulsive, the system supports the two (duality-related) gapped phases reminiscent of the clean Ising model, separated by a mixed phase where segments of phase-locked rungs are embedded in a background of charge-locked rungs or vice versa.

Our findings suggest that engineered Josephson ladders in the strong quantum-fluctuations regime ($E_C \sim E_J$) can serve as a compelling platform for simulating the physics of the random-field Ising model, as well as coupled boson-fermion systems in 1D—as long as they possess the above mentioned $\mathbb{Z}_2$ symmetry. Moreover, provided separate contacts to the edges of the two legs are accessible, probing of the various phases is possible via measurement of different conductance components [23]. In practice, accurate control of the parameters in Josephson arrays which ensures a perfect symmetry is quite challenging. However, as long as symmetry-breaking corrections are small, they do not affect the model qualitatively. We note that the effect of uniform $\mathbb{Z}_2$-symmetry breaking terms was discussed in earlier literature, showing that they can be accounted for perturbatively. Specifically, small corrections to the quadratic terms are marginal [23,34]. A more relevant perturbation is imposed by a uniform voltage bias between the two legs, which (following a duality transformation) is equivalent to a perpendicular magnetic field as introduced in Ref. [22]. Once again, there is a range of stability where such corrections merely shift the critical lines but the phase diagram maintains its structure. The random counterparts of the above mentioned terms are less relevant. We therefore conclude that a weakly broken $\mathbb{Z}_2$ symmetry will not affect our main results, save for quantitative modifications (e.g., the CDW phase in Fig. 1 will somewhat shrink).

An alternative realization of the model, which allows us to better control and even fully guarantee the $\mathbb{Z}_2$ symmetry, can potentially be achieved in a platform where the discrete degree of freedom is not spatial but rather some internal degree of freedom (e.g., a spin, valley, or orbital index). The most promising candidate is a (bosonic) cold atom system, where a "synthetic dimension" is introduced via manipulations of internal degrees of freedom of the atoms [35–37]. Another suggestive platform can be served by van der Waals materials with long-range disorder, where valley symmetry can be controlled to a reasonable degree. Such realization in bilayer graphene subjected to a strong magnetic field was discussed in Ref. [23]. The rapid progress in design and fabrication of hybrid layered material in recent years offers a richer variety of systems with suitable ingredients, e.g., a graphene-black phosphorus bilayer, which exhibits a nearly flat quasi-1D band structure [38]; a design of realizations for our model in such platforms is left for future studies.

As a concluding remark, it would be interesting to test our results and their limitations in a numerical study. For that purpose, it would be useful to utilize an equivalent lattice model efficiently tractable by standard numerical methods such as classical Monte Carlo or density matrix renormalization group (DMRG). We propose two general routes to this end: First, it is possible to map our quantum model into an equivalent classical spin model in 2D and address it in Monte Carlo, similarly to the study of a single Josephson chain [39]. An alternative route could be mapping to a model of interacting-fermions ladder, where competing interactions can be tuned to generate emergent bosons (tightly-bound pairs) with repulsive interactions. Such models are tractable by DMRG—see, e.g., Refs. [40,41] (in the latter, compelling evidence for the Ising transition of the clean limit was already seen).

ACKNOWLEDGMENTS

We gratefully acknowledge useful discussions with Ehud Altman, Ganpathy Murthy, Jonathan Ruhman, and Thomas Vojta. E.S. thanks the Aspen Center for Physics (NSF Grant No. 1066293) for its hospitality. This work was supported by the US-Israel Binational Science Foundation through Awards No. 2016130 and No. 2018726, and by the Israel Science Foundation (ISF) Grant No. 993/19.

APPENDIX A: DERIVATION OF THE LOW-ENERGY THEORY

The ladder model in the clean limit is described in Eqs. (1)–(3). In this Appendix we detail the derivation of its low-energy approximation, Eqs. (6)–(8), used as a basis for the remains of the analysis.

As a first stage, in the definition of ρ_ν in terms of θ_ν [Eq. (4)] we keep only the leading harmonics, coming from $p = \pm 1$. The Hamiltonian acquires the structure

$$\begin{aligned}\mathcal{H}_\nu &= \frac{U}{2\pi^2}(\partial_x\theta_\nu)^2 + \frac{\rho_s}{2}(\partial_x\phi_\nu) - \frac{2\rho_0 U}{\pi}\partial_x\theta_\nu\cos\left(2(\theta_\nu - \pi\rho_0 x)\right) + 2U\rho_0^2\cos\left(2(\theta_\nu - \pi\rho_0 x)\right)^2\\ \mathcal{H}_{\rm int} &= \frac{V}{\pi^2}\partial_x\theta_1\partial_x\theta_2 - \frac{2\rho_0 V}{\pi}[\partial_x\theta_1\cos\left(2(\theta_2 - \pi\rho_0 x)\right) + \partial_x\theta_2\cos\left(2(\theta_1 - \pi\rho_0 x)\right)]\\ &\quad + 4\rho_0^2 V\cos\left(2(\theta_1 - \pi\rho_0 x)\right)\cos\left(2(\theta_2 - \pi\rho_0 x)\right).\end{aligned} \tag{A1}$$

The terms combining gradients with cosines must vanish, as they are not symmetric to inversion ($x \mapsto -x$). We rewrite Eq. (A1) in terms of $\theta_\pm, \phi_\pm$ as defined in Eq. (5), describing the symmetric (+) and antisymmetric (−) sectors to get the following Hamiltonian:

$$\begin{aligned}H = \int dx\Bigg[&\frac{U+V}{2\pi^2}(\partial_x\theta_+)^2 + \frac{\rho_s}{2}(\partial_x\phi_+)^2 + 2\rho_0^2 V\cos(\sqrt{8}\theta_+ - 4\pi\rho_0 x)\\ &+ \frac{U-V}{2}(\partial_x\theta_-)^2 + \frac{\rho_s}{2}(\partial_x\phi_-)^2 + 2\rho_0^2 V\cos(\sqrt{8}\theta_-) - J\cos(\sqrt{2}\phi_-)\\ &+ U\rho_0^2\cos(\sqrt{8}\theta_+ + \sqrt{8}\theta_- - 4\pi\rho_0 x) + U\rho_0^2\cos(\sqrt{8}\theta_+ - \sqrt{8}\theta_- - 4\pi\rho_0 x)\Bigg].\end{aligned} \tag{A2}$$

The first two lines correspond to Eqs. (6) and (7) in the main text. The terms on the third line are less relevant, being higher harmonics which we already neglect in the density operator ρ_ν.

We now identify the quadratic part of each sector as a Luttinger liquid, with $u_\pm = \sqrt{(U \pm V)\rho_s}$ and $K_\pm = \sqrt{\frac{U\pm V}{\pi^2\rho_s}}$. We see that for the bare values, $K_+ > K_-$ for repulsive interactions, and $K_+ < K_-$ for attractive interactions. However, as we show in Appendix C 2, disorder terms of the type $\mathcal{D}_{U/s}$ modify each of these parameters independently; therefore, this hierarchy of the Luttinger parameters is not necessarily maintained once disorder is introduced.

To further analyze the antisymmetric sector, a slight modification of the standard fermionization [30] is helpful:

$$\psi_r = \frac{U_r}{\sqrt{2\pi a}}e^{-i[r\phi_-(x)/\sqrt{2} - \sqrt{2}\theta_-(x)]} \tag{A3}$$

with $r = R, L$ for right- and left-moving fermions, a the lattice constant, and U_r the Klein factor. For $K_- = 2$, one can exactly map Eq. (7) to noninteracting fermions:

$$\begin{aligned}\psi_R^\dagger(-i\partial_x)\psi_R - \psi_L^\dagger(-i\partial_x)\psi_L &= \frac{2(\partial_x\theta_-)^2 + \frac{(\partial_x\phi_-)^2}{2}}{\pi}\\ \psi_R^\dagger\psi_L + \text{H.c.} &= \frac{1}{\pi a}\cos(\sqrt{2}\phi_-)\\ \psi_L\psi_R + \text{H.c.} &= \frac{1}{\pi a}\cos(\sqrt{8}\theta_-).\end{aligned} \tag{A4}$$

Now one can decompose these fermions to Majorana (real) fields

$$\psi_r = \frac{\xi_{r1} + i\xi_{r2}}{\sqrt{2}} \tag{A5}$$

and the Hamiltonian decouples into two independent sectors: one with $\xi_{\uparrow R} \equiv \xi_{1R}$ and $\xi_{\uparrow L} \equiv \xi_{2L}$, and the other with $\xi_{\downarrow R} \equiv \xi_{2R}$ and $\xi_{\downarrow L} \equiv \xi_{1L}$. The Hamiltonian in terms of these Majorana fields is

$$\begin{aligned}H = \sum_{\nu=\updownarrow}\int dx u_-[&\xi_{R\nu}(-i\partial_x)\xi_{R\nu} - \xi_{L\nu}(-i\partial_x)\xi_{L\nu}]\\ &- i\Delta_\nu\xi_{R\nu}\xi_{L\nu}.\end{aligned} \tag{A6}$$

In the case of $K_- = 2$, $\Delta_\updownarrow = \Delta_\theta \pm \Delta_\phi$ where $\Delta_{\theta,\phi}$ are linear in $g_{\theta,\phi}$, the coefficients of the cosines in Eq. (7). However, if $K_- \neq 2$, there is an interaction term $\propto (K_- - 2)\xi_{\uparrow R}\xi_{\uparrow L}\xi_{\downarrow R}\xi_{\downarrow L}$. Provided there is a separation of energy scales between the $\updownarrow$ sectors, this can be treated in mean field; the effective gaps have the same structure but with $\Delta_{\theta,\phi}$ the gap of the corresponding sine-Gordon model. This approximation is self-consistent if $\Delta_\theta \approx \Delta_\phi$ ($\Delta_\downarrow \ll \Delta_\uparrow$), in which case integrating over the $\uparrow$ sector is justified and yields the low-energy theory. In this case, the effective Hamiltonian is dominated by the sector with the smaller gap $\Delta_\downarrow$ [Eq. (8) in the main text where we have dropped the subscript $\downarrow$ on Δ], which undergoes a transition as $\Delta_\downarrow$ changes sign. This allows us to analyze the behavior of the transition in the antisymmetric sector and identify it as an Ising transition [23]. Note that $\Delta_\uparrow$ and $\Delta_\downarrow$ change their classification when the

interaction term $g_\theta \propto V$ changes its sign; we define them such that $|\Delta_\uparrow| = |\Delta_\theta| + |\Delta_\phi|$ and so $\Delta_\uparrow$ is always the larger in magnitude.

We next derive the disorder term H_η originating from randomness in the chemical potential $\mu(x)$. Assuming a perfect symmetry between the legs and employing the leading harmonics in the expansion Eq. (4), the coupling to $\mu(x)$ is given by

$$\begin{aligned} H_\mu &= -\int dx\mu(x)[\rho_1(x)+\rho_2(x)] \\ &= \int dx\mu(x)\Big[\frac{1}{\pi}(\partial_x\theta_1+\partial_x\theta_2) \\ &\quad -2\rho_0(\cos(2\theta_1-2\pi\rho_0 x)-\cos(2\theta_2-2\pi\rho_0 x))\Big] \\ &= \int dx\frac{\sqrt{2}\mu(x)}{\pi}\partial_x\theta_+ \\ &\quad -\int dx 4\rho_0\mu(x)\cos(\sqrt{2}\theta_+-2\pi\rho_0 x)\cos(\sqrt{2}\theta_-). \end{aligned} \tag{A7}$$

The first term can be "gauged out" with the shift by a random phase:

$$\theta_+ \mapsto \theta_+ + \varphi(x), \quad \varphi(x) \equiv \frac{\sqrt{2}\pi}{(U+V)}\int^x \mu(x) \tag{A8}$$

which yields

$$\cos(\sqrt{8}\theta_+ - 4\pi\rho_0 x) \mapsto \tfrac{1}{2}e^{i(\sqrt{8}\theta_+ - 4\pi\rho_0 x+\sqrt{8}\varphi(x))} + \text{H.c.} \tag{A9}$$

Substituting in the cosine of Eq. (6), we obtain

$$2\rho_0^2 V e^{i(\sqrt{8}\varphi(x)-4\pi\rho_0 x)} \equiv \delta g(x), \tag{A10}$$

where the correlations of δg are approximated to be totally noncorrelated. Note that the amplitude g might also change because of randomness in V.

The second term of H_μ [Eq. (A7)] is different. With the random phase from the first term, we can write it as

$$\begin{aligned} H_\eta &= \int dx[\eta(x)e^{i\sqrt{2}\theta_+} + \text{H.c.}]\cos(\sqrt{2}\theta_-), \\ \eta(x) &\equiv 4\rho_0\mu(x)e^{i(\sqrt{2}\varphi(x)-2\pi\rho_0 x)}. \end{aligned} \tag{A11}$$

Here $\eta(x)$ has both random amplitude and random phase, so we once again approximate it to be totally noncorrelated.

APPENDIX B: DERIVATION OF THE RG EQUATIONS

In this Appendix we will discuss the method used to derive the RG equations in this work, presented in Sec. III. We particularly focus on the contribution of the disorder term in chemical potential ($\mathcal{D}_\eta$) in different regimes of the parameter space, primarily on the regime where the antisymmetric sector is well described by Majorana fields.

Generally, we consider a disorder term with the operator $\hat{O}(x,\tau)$ of the form

$$S_{\text{dis}} = \int dxd\tau[\delta g_O(x)\hat{O}(x,\tau)] \tag{B1}$$

in which the random coefficient $\delta g_O(x)$ obeys $\langle\langle \delta g_O\rangle\rangle = 0$ and the short-range correlations:

$$\langle\langle \delta g_O(x)\delta g_O(x')\rangle\rangle = D_O\delta(x-x'), \tag{B2}$$

where $\langle\langle\cdots\rangle\rangle$ stands for statistical averaging over the realizations of the disorder. We substitute this as a term in the action, write the expression for the partition function, and expand to second order in S_{dis}. Averaging over disorder and using Eq. (B2) leads to the main contribution:

$$\left\langle\left\langle S_{\text{dis}}^2\right\rangle\right\rangle = \int dxd\tau d\tau' D_O\hat{O}(x,\tau)\hat{O}(x,\tau') \tag{B3}$$

and one should subtract the disconnected terms, resulting from $\langle\langle S_{\text{dis}}\rangle\rangle^2$.

To derive RG equations, we write the action describing our model in momentum space. Now we would like to apply momentum-sell renormalization group, so we begin by introducing a high momentum cutoff Λ and splitting the fields representing the free part of the action to their slow and fast momentum components:

$$\begin{aligned} \xi(r) &= \xi^<(r) + \xi^>(r) \\ \xi^<(r) &= \frac{1}{\sqrt{L\beta}}\sum_{||q||<\Lambda'} e^{iq\cdot r}\xi(q) \\ \xi^>(r) &= \frac{1}{\sqrt{L\beta}}\sum_{\Lambda'<||q||<\Lambda} e^{iq\cdot r}\xi(q), \end{aligned} \tag{B4}$$

where ξ stands for either of the Majorana fields ξ_R, ξ_L or the bosonic fields ϕ_+, θ_+; here $\Lambda' = e^{-d\ell}\Lambda$ is a slightly smaller momentum cutoff, $q = (\frac{\omega}{u}, k)$, $r = (u\tau, x)$, and $||q||^2 = \frac{\omega^2}{u^2} + k^2$ with the appropriate velocity u; L and β are, respectively, the length of the system and the inverse temperature.

If the operator $\hat{O}(x,\tau)$ can be directly written in terms of the fields in the free action, in our case $\theta_+, \phi_+, \xi_R, \xi_L$, one can integrate over the fast modes $(\theta_+^>, \phi_+^>, \xi_R^>, \xi_L^>)$ to get an effective expression for the action of the slow modes. Below we demonstrate how this procedure can be implemented and show that this effective expression can be cast in the following form:

$$\begin{aligned} &\int dxd\tau d\tau' e^{\gamma d\ell}D_O\hat{O}^<(x,\tau)\hat{O}^<(x,\tau') \\ &\quad + \sum_i \int dxd\tau\alpha_i d\ell\hat{O}_i^<(x,\tau), \end{aligned} \tag{B5}$$

where $\{\hat{O}_i\}$ is a set of local operators and α_i are coefficients proportional to D_O; the exponent γ is related to the scaling dimension of $\hat{O}$; finally, $\hat{O}^<$ is just $\hat{O}$ with all the fields replaced with their "slow" low-momentum component.

This effective action is defined to fulfill the following equation:

$$e^{-S_{\text{eff}}^<} = \int \mathcal{D}\xi^> e^{-S}, \tag{B6}$$

where we integrate over fast modes of all fields. To obtain $S_{\text{eff}}^<$, we expand the exponent around the quadratic part of the action S_0, which results with a perturbative description of the way D_O scales and its effects on the other parameters of the model.

We begin with a simple example, the case of Δ disorder [Eqs. (8) and (12)], where $\delta g_O(x) = \delta\Delta(x)$ and $\hat{O} = i\xi_R\xi_L$. The disorder-averaged expression for $S^2_{\rm dis}$ is then given by

$$\begin{aligned}\langle\langle S^2_{\rm dis}\rangle\rangle &= -D_\Delta \int dx d\tau d\tau' \xi_R(x,\tau)\xi_L(x,\tau)\xi_R(x,\tau')\xi_L(x,\tau') \\ &= -D_\Delta \int d^3k d^2\omega \xi_R(k_1,\omega_1)\xi_L(k_2,-\omega_1)\xi_R(k_3,\omega_3)\xi_L(-k_1-k_2-k_3,-\omega_3). \end{aligned} \tag{B7}$$

In momentum space we split the five-dimensional integral to different regimes according to the decomposition in Eq. (B4). That means the integration regime is split into sixteen different parts, as each momentum vector can be in the smaller ball ($|q| < \Lambda'$, "slow") or on the momentum shell ($\Lambda' < |q| < \Lambda$, "fast"). However, expectation values over an odd number of fields vanish, which means a large part of the terms cancel. Among those remaining we can use some symmetries and essentially get the following expression:

$$\begin{aligned}\langle\langle\langle S^2_\Delta\rangle_>\rangle\rangle &= -L\beta D_\Delta \int d^5q \xi_R\xi_L\xi_R\xi_L - 2\beta D_\Delta \int dk d\omega \xi_R(k,\omega)\xi_L(-k,-\omega) \oint dk' d\omega' \langle \xi_R(k',\omega')\xi_L(-k',-\omega')\rangle_> \\ &\quad - 2D_\Delta \int dk d\omega \xi_R(k,\omega)\xi_L(-k,-\omega) \oint dk' \langle \xi_L(k',-\omega)\xi_R(-k',\omega)\rangle_> \\ &\quad + D_\Delta \int dk d\omega \xi_R(k,\omega)\xi_R(-k,-\omega) \oint dk' \langle \xi_L(k',\omega)\xi_L(-k',-\omega)\rangle_> \\ &\quad + D_\Delta \int dk d\omega \xi_L(k,\omega)\xi_L(-k,-\omega) \oint dk' \langle \xi_R(k',\omega)\xi_R(-k',-\omega)\rangle_> - L\beta \oint d^5q \langle \xi_R\xi_L\xi_R\xi_L\rangle_>, \end{aligned} \tag{B8}$$

where $d^5q = dk_1dk_2dk_3d\omega_1d\omega_3$, and the integrals $\int dk$ and $\int d\omega$ are over the smaller momentum ball $|q_i| < \Lambda'$, while those denoted by $\oint dkd\omega'$ are over the shell; $\oint dk'$ means that (k',ω) should be on the momentum shell. Also, note we have used the fact that $\langle \xi(q)\xi(-q')\rangle = f(q)\delta_{q,q'}$.

Among the resulting six terms, the first one will give us the rescaling of D_Δ, the next four will be corrections to local terms like the second line of Eq. (B5), and the last one is a noninteresting constant. The expectation values are all over fast modes and with respect to the quadratic action S_- (the antisymmetric part of S_0). They are known, and using the approximation $\omega/u_-, k \ll \Lambda$ all the integrals are quite simple as well.

We now note that Eq. (B8) yields the desired correction to $S^<_{\rm eff}$ [Eq. (B6)] only after re-exponentiating. To leading order in D_Δ, the correction is given by $\frac{1}{2}(\langle S^2_{\rm dis}\rangle - \langle S_{\rm dis}\rangle^2)$ where the disconnected terms cancel. After performing the integrals over the momentum shell and transforming back to the real-space representation, we obtain

$$\begin{aligned}\frac{\langle\langle\langle S^2_{\rm dis}\rangle_>\rangle\rangle - \langle\langle\langle S_{\rm dis}\rangle^2_>\rangle\rangle}{2} &= -\frac{D_\Delta}{2}\int dx d\tau d\tau' \xi^<_R(\tau)\xi^<_L(\tau)\xi^<_R(\tau')\xi^<_L(\tau') - \frac{2D_\Delta\Delta}{u_-^2(1+(\Delta/u_-\Lambda)^2)}\left(\frac{1}{\Lambda'}-\frac{1}{\Lambda}\right)\int dx d\tau i\xi^<_R\xi^<_L \\ &\quad - \frac{D_\Delta}{2u_-^2(1+(\Delta/u_-\Lambda)^2)}\left(\frac{1}{\Lambda'}-\frac{1}{\Lambda}\right)\int dx d\tau (\xi^<_R\partial_\tau\xi^<_R + \xi^<_L\partial_\tau\xi^<_L). \end{aligned} \tag{B9}$$

The last step in the RG procedure is to rescale the coordinates and fields. In momentum space, we rewrite $q \mapsto qe^{d\ell}$ for q to restore the original cutoff Λ. The differentials $dx, d\tau$ correspondingly are multiplied by a factor $e^{d\ell}$ each, and ξ are multiplied by $e^{y_\xi d\ell}$ where y_ξ is their scaling dimension. In the clean model, $y_\xi = -\frac{1}{2}$; however, here there is a correction of order D_Δ required to compensate for the last term in Eq. (B9), adjusting the overall coefficient of the term $\xi\partial_\tau\xi$ in the effective action to have a coefficient unity. Substituting these rescaling factors, the leading term with coupling to four fermion fields becomes

$$e^{(3+4y_\xi)d\ell} D_\Delta \int dx d\tau d\tau' \xi_R(x,\tau)\xi_L(x,\tau)\xi_R(x,\tau')\xi_L(x,\tau') \tag{B10}$$

which gives the RG equation for D_Δ. The equations for Δ and u_- arise from the appropriate rescaling of the fields and coordinates in the last two terms of (B9). This concludes our derivation of Eq. (21) in the main text.

The above derivation relied on the ability to switch between real space and momentum space in a straightforward manner. This is useful for additional disorder terms that are quadratic in the free fields of S_0, such as $\delta U(x)(\partial_x\theta_+)^2$ in the symmetric sector. However, when there are nonquadratic operators involved, the procedure is more complicated as the coupling between fast and slow fields is tighter, and a simple representation of $\hat{O}$ in (k,ω) space is lacking.

To deal with this type of disorder terms, certain approximations will need to be implemented in the procedure of integrating the fast modes. We employ the strategy described below for a general disorder term. Subsequently, we apply this approach to analyze the chemical potential disorder term H_η [Eq. (13)].

We begin by splitting the double-time integral of Eq. (B3) to two different terms, $\tau \approx \tau'$ and $\tau \not\approx \tau'$, where the former

accounts for time differences $\Delta\tau \equiv \tau - \tau'$ within the short-time cutoff $(u\Lambda)^{-1}$:

$$S^2_{\rm dis} = \int_{\tau \not\approx \tau'} dx d\tau d\tau' D_O \hat{O}(x,\tau)\hat{O}(x,\tau') + \int_{\tau \approx \tau'} dx d\tau d\tau' D_O \hat{O}(x,\tau)\hat{O}(x,\tau'). \quad \text{(B11)}$$

Generally, different local operators $\hat{O}_i$ are generated from local expansions of the term $\hat{O}(x,\tau')$:

$$\hat{O}(x,\tau') = \hat{O}(x,\tau) + (\Delta\tau)\partial_\tau \hat{O}(x,\tau) + \cdots . \quad \text{(B12)}$$

One can expand to leading orders in $\Delta\tau$, resulting in a set of local operators (independent of τ') multiplied by some function of $\Delta\tau$:

$$S^2_{\rm dis} = \int_{\tau \not\approx \tau'} dx d\tau d\tau' D_O \hat{O}(x,\tau)\hat{O}(x,\tau') + \sum_i \int_{\tau \approx \tau'} dx d\tau d(\Delta\tau) D_O F_i(\Delta\tau)\hat{O}_i(x,\tau). \quad \text{(B13)}$$

We now turn to integrating over the fast modes. In the first term, we know that the correlation of the fast modes $\langle \hat{O}^>(\tau)\hat{O}^>(\tau')\rangle$ decays, so that under the approximation $\tau \not\approx \tau'$ averaging over the fast modes will not depend on $\Delta\tau$. The second term is already composed only from local terms by construction. We therefore only need to calculate local expectation values. The result can be brought to the following structure:

$$S^{<2}_{\rm dis} = e^{\gamma_O d\ell} \int_{\tau \not\approx \tau'} dx d\tau d\tau' D_O \hat{O}^<(x,\tau)\hat{O}^<(x,\tau') + \sum_i e^{\gamma_i d\ell} \int_{\tau \approx \tau'} dx d\tau d(\Delta\tau) D_O F_i(\Delta\tau)\hat{O}^<_i(x,\tau), \quad \text{(B14)}$$

where γ_i and γ_O are related to the scaling dimensions of the operators, as will be seen in what follows.

To restore back the effective $S^2_{\rm dis}$ in the slow modes sector to the form of (B5), one must unite the $\tau \not\approx \tau'$ and $\tau \approx \tau'$ contributions to one term. A part of the local term is "absorbed" back in the nonlocal term to reconstruct the structure of a disorder term. Following integration over $\Delta\tau$ we obtain

$$S^{<2}_{\rm dis} = e^{\gamma_O d\ell} \int dx d\tau d\tau' D_O \hat{O}^<(x,\tau)\hat{O}^<(x,\tau') + \sum_i (e^{\gamma_i d\ell} - e^{\gamma_O d\ell}) \int dx d\tau D_O C_i \hat{O}^<_i(x,\tau), \quad \text{(B15)}$$

where $C_i \equiv \int d(\Delta\tau) F_i(\Delta\tau)$, in which the integral is bounded by the cutoff $(u\Lambda)^{-1}$ and yields a nonuniversal constant. The exact value of C_i is not important—only its sign and dependence on the parameters of the model. Note that $e^{\gamma_i d\ell} - e^{\gamma_O d\ell} \approx (\gamma_i - \gamma_O)d\ell$, so this can be understood as a correction to the coefficient of $\hat{O}_i$ (an operator that typically exists in the free action S_0) of order $d\ell$.

To complete the RG transformation, we have to restore the cutoff Λ. Similarly to the discussion of the quadratic case, dx and $d\tau$ will each be multiplied by a factor of $e^{d\ell}$. In the limit $d\ell \to 0$, this rescaling can be neglected in the second line of Eq. (B15). However, in the first, nonlocal term it yields an overall prefactor $e^{(3+\gamma_O)d\ell}$; we interpret the resulting coefficient as the renormalized disorder. Noting that $\gamma_O < 0$, the exponent $y_{D_O} \equiv 3 + \gamma_O$ is the scaling dimension of the disorder operator, which will determine the condition for it to be relevant. The second, local term provides a set of corrections to the parameters of S_0.

The last step is re-exponentiation—once again leading to subtraction of the disconnected term $\langle S_{\rm dis}\rangle^2$. This yields the final form Eq. (B5).

To demonstrate the general procedure described above, we now briefly review the analysis the disorder term H_g [Eq. (10)]. The operator in this case is $\hat{O} = \cos\sqrt{8}\theta_+$. We will use intermediate calculations that match Appendix E of Ref. [30], and the final result will be identical to Ref. [33]. Averaging over the fast modes we have

$$\langle \hat{O}(x,\tau)\rangle_> = e^{-\frac{2}{K}} \hat{O}^<(x,\tau) \quad \text{(B16)}$$

and therefore $\gamma_O = -\frac{4}{K}$, so the scaling of D_g is $\frac{dD_g}{d\ell} = (3 - \frac{4}{K})D_g$.

Looking at the short-range regime $\tau \approx \tau'$, the product $\hat{O}(\tau)\hat{O}(\tau')$ can be simplified using trigonometrical identities and the expansion Eq. (B12). The result yields two local terms in the leading orders:

$$\hat{O}_1(\tau) = \cos\sqrt{32}\theta_+$$
$$\hat{O}_2(\tau) = (\partial_\tau\theta_+)^2. \quad \text{(B17)}$$

The operator $\hat{O}_1$ is not very interesting, as its dimension is very low, $2 - \frac{8}{K}$, and so it is irrelevant in our regime of interest. The operator $\hat{O}_2$, on the other hand, will lead to the corrections to u_+ and K_+ as they appear in (24) and (25).

We next turn to apply this approach for the analysis of H_η [Eq. (13)], where $\hat{O} = \cos(\sqrt{2}\theta_+)\cos(\sqrt{2}\theta_-)$. As we follow the same procedure, to linear order in D_η one straightforwardly obtains the corrections to various terms which couple to local operators $\hat{O}_i$. However, the RG transformation of the disorder term itself poses a challenge: As long as the gap Δ in the antisymmetric sector is finite, the correlations of $\cos(\sqrt{2}\theta_-)$ never decay as a power law for $\Delta\tau \to \infty$. Rather, employing the decomposition

$$\cos\sqrt{2}\theta_- = \langle\cos\sqrt{2}\theta_-\rangle + :\cos\sqrt{2}\theta_-: \quad \text{(B18)}$$

the second term has exponentially decaying correlations. For $V > 0$, the first term vanishes ($\cos\sqrt{2}\theta_-$ couples to the disorder field in the Ising representation [32]); hence $\hat{O}$ is exponentially irrelevant to the present order in the perturbative expansion of H_η.

To derive RG flow equations for D_η, we therefore need to consider the next order in the perturbative expansion. This yields a disorder term coupling to the operator $\cos\sqrt{8}\theta_-$, which has a simple representation in terms of either the fermion fields $\xi_{R,L}$ or the massive bosonic field θ_-. Indeed, the fourth order term $S^4_{\rm dis}$ (with a coefficient proportional to D^2_η) contains a specific *four-point* combination $\hat{O}(x,\tau)\hat{O}(x,\tau)\hat{O}(x,\tau')\hat{O}(x,\tau')$ which possesses power-law decaying correlations. Using $\cos^2(\sqrt{2}\theta_-) = \frac{1}{2}[1 + \cos(\sqrt{8}\theta_-)]$, this contributes several terms: Some of them are local and can be interpreted as corrections to δ and g

(the latter renormalizing D_g as well); the leading nonlocal ("disorderlike") term is therefore associated with the operator $\hat{\tilde{O}} = \cos(\sqrt{8}\theta_+(x,\tau))\cos(\sqrt{8}\theta_-(x,\tau))$, with a coefficient $\propto D_\eta^2$.

Proceeding with the analysis of the latter disorder term is made possible by implementing the approximate representation of $\cos(\sqrt{8}\theta_\pm)$ in terms of the free fields and explicitly evaluating $\langle\,\rangle_>$. In particular, the operator $\cos(\sqrt{8}\theta_+)$ is already included in H_g and yields the same scaling exponent; the scaling dimension of $\cos(\sqrt{8}\theta_-)$ can be inferred from either the fermionic or the massive bosonic representations, depending on the value of K_- (see main text). This yields the following scaling dimensions:

$$y_{D_\eta} = \begin{cases} \frac{1}{2} - \frac{2}{K_+} & \text{fermionic behavior} \\ \frac{3}{2} - \frac{2}{K_+} - \frac{2}{K_-(1+\delta^2)} & \text{bosonic behavior} \end{cases} \tag{B19}$$

with δ the dimensionless gap in the bosonic regime. Note that in any case, D_η is always less relevant than D_g; hence the emergence of a disordered insulating phase is dominated by the critical value of D_g and is only indirectly dependent on D_η via the corrections it generates to the other parameters.

We now comment on the contribution to the RG equations coming from linear order in D_η. These arise from corrections to the coefficients of the following local operators $\{\hat{O}_i\}$:

$$\begin{aligned} \hat{O}_1(\tau) &= (\partial_\tau\theta_+)^2 \\ \hat{O}_2(\tau) &= \cos\sqrt{8}\theta_- \\ \hat{O}_3(\tau) &= (\partial_\tau\theta_-)^2 \end{aligned} \tag{B20}$$

these result in the contribution of $\mathcal{D}_\eta$ to Eqs. (24) and (25).

We finally note that in the regime where the antisymmetric sector is a gapped superconductor, any operator which contains nontrivial factors of $\cos\gamma\theta_-$ (with arbitrary γ) is exponentially irrelevant and contributes nothing to any order in D_η. The only contributions come from terms in the expansion that couple only to θ_+, and therefore, at least to leading (second) order, the effect of D_η is just creating a shift in D_g:

$$D_g \to D_g^{\text{eff}} = D_g + \alpha D_\eta^2. \tag{B21}$$

For this reason, deep in the SC phase H_η can be ignored altogether and the $\pm$ sectors are effectively decoupled.

APPENDIX C: ANALYTIC SOLUTIONS OF THE RG EQUATIONS

The set of equations described in Eq. (25) is coupled, and an analytic solution will be complicated if it even exists. However, some special cases can be helpful to understand the type of flow expected in each phase.

1. Quadratic Disorder

As discussed in Sec. III A of the main text, the disorder in quadratic terms of the symmetric (gapless) sector $\delta U(x)(\partial_x\theta_+)^2$, $\delta\rho_s(x)(\partial_x\phi_+)^2$ is always irrelevant, and therefore we have not discussed it in detail in the main text. However, in the presence of this disorder alone one can exactly solve the equations and understand its effect on the system.

The equations for the disorder itself are simple:

$$\frac{d\mathcal{D}_{U/s}}{d\ell} = -\mathcal{D}_{U/s} \tag{C1}$$

so the solution is just an exponent

$$\mathcal{D}_{U/s}(\ell) = \mathcal{D}^0_{U/s}e^{-\ell}. \tag{C2}$$

This can be substituted in the equations for K_+, u_+:

$$\begin{aligned} \frac{dK_+}{d\ell} &= 4\left(\mathcal{D}^0_s K_+^2 - \frac{\mathcal{D}^0_U}{K_+^2}\right)e^{-\ell}K_+ \\ \frac{du_+}{d\ell} &= -4\left(\mathcal{D}^0_s K_+^2 + \frac{\mathcal{D}^0_U}{K_+^2}\right)e^{-\ell}u_+. \end{aligned} \tag{C3}$$

Generally solving these equations is hard, but to leading order in $\mathcal{D}_{U/s}$ the renormalization of K_+ inside the round brackets can be neglected. The resulting flow is of the form $\frac{dQ}{d\ell} = Ae^{-\ell}Q$, with the solution $Q(\ell) = Q_0 e^{A\cdot(1-e^{-\ell})}$. The asymptotic values (at $\ell \to \infty$) are

$$\begin{aligned} u_+(\infty) &= u_+ e^{-4(\mathcal{D}^0_s K_+^2 + \frac{\mathcal{D}^0_U}{K_+^2})} \\ K_+(\infty) &= K_+ e^{4(\mathcal{D}^0_s K_+^2 - \frac{\mathcal{D}^0_U}{K_+^2})}. \end{aligned} \tag{C4}$$

As this flow converges very fast, we generally ignored it and assumed the values of K_+ and u_+ we were using are the stable ones (in terms of $\mathcal{D}_{U/s}$).

One should also consider the effect of these disorder terms on the antisymmetric sector. Generally the effect should be similar but adding a factor of $(1+\delta^2)$ complicates the calculations. We can note that qualitatively, the effect on the antisymmetric sector will be weaker. This is what gives us the option to tune the ratio $\frac{K_+}{K_-}$ to be above or below 1, independently of the sign of V (which does constrain the bare values)—a strong $\mathcal{D}_s$ term will push the ratio up, and a strong $\mathcal{D}_U$ term will push it down.

2. Antisymmetric Sector

The disorder in Δ in the antisymmetric sector is special, as $\mathcal{D}_-$ always diverges: $\frac{d\mathcal{D}_-}{d\ell} > \mathcal{D}_-$, which indicates an exponential divergence. Yet, there is an ordered phase in the sector: As $\mathcal{D}_-$ is the variance in the dimensionless gap δ, if $\sqrt{\mathcal{D}_-} \ll \delta$ the randomness in the gap is actually small compared to the average gap δ, and the clean limit is effectively recovered. Indeed, in the RG equations $\mathcal{D}_-$ is always divided by $1+\delta^2$.

As diverging $\mathcal{D}_-$ is not a good indicator for the nature of the phase, one should look instead on the "normalized disorder" parameter $\tilde{\mathcal{D}}_- = \frac{\mathcal{D}_-}{1+\delta^2}$ defined in Sec. III B, which obeys Eq. (22) in the case $\mathcal{D}_\eta = 0$. The RG equations for the velocity u_- and δ become

$$\frac{du_-}{d\ell} = -\tilde{\mathcal{D}}_- u_-, \qquad \frac{d\delta}{d\ell} = (1 - 2\tilde{\mathcal{D}}_-)\delta. \tag{C5}$$

Therefore, diverging $\tilde{\mathcal{D}}_-$ will lead to $u_-, \delta \to 0$, which characterizes a disordered phase. However, from Eq. (22) it is clear that $\tilde{\mathcal{D}}_- = \frac{3}{16}$ is a turning point. If $\tilde{\mathcal{D}}_- > \frac{3}{16}$, $\frac{d\tilde{\mathcal{D}}_-}{d\ell} > 0$ and the disorder will diverge. On the other hand, if $\tilde{\mathcal{D}}_- < \frac{3}{16}$, there is

a critical value of δ above which $\tilde{\mathcal{D}}_-$ will flow downwards and turn irrelevant: $\delta_c = \frac{1}{1-16/3\tilde{\mathcal{D}}_-}$.

As a rule of thumb, for low initial values there is no strong coupling between δ and $\tilde{\mathcal{D}}_-$ (no linear contributions from one parameter on the other) and the main question is what will happen first—either δ will reach a value of order 1 or $\tilde{\mathcal{D}}_-$ will approach the critical value $\frac{3}{16}$ or close to it. As δ and $\tilde{\mathcal{D}}_-$ scale the same close to the point ($\delta = 0, \tilde{\mathcal{D}}_- = 0$), one expects linear critical lines yielding the V shape $\tilde{\mathcal{D}}_- \propto |\delta|$, as can be seen in Fig. 2. We finally note that to get the right panel of this figure, one may use the explicit K_- dependence of Δ (e.g., Eq. (D2) or Eqs. (25)–(27) in [23]); this leads to the curving of the phase boundary in the top and bottom of the figure.

APPENDIX D: BOSONS WITH A RANDOM MASS

In this Appendix we consider a type of disorder which was not discussed in the main text: randomness in the gap characterizing the massive bosonic regimes of the antisymmetric sector. Specifically, deep in the superconducting phase, one can write the following effective Hamiltonian to describe fluctuations in the relative phase ϕ_-:

$$H_- = \frac{u_-}{2\pi}\int dx\left[K_-(\partial_x\theta_-) + \frac{1}{K_-}(\partial_x\phi_-)^2 + \Delta^2\phi_-^2\right], \quad \text{(D1)}$$

where we have replaced $g_\phi \cos\phi_-$ with the gap term $\Delta^2\phi_-^2$ following the gap equation for a sine-Gordon model [30]:

$$\frac{\Delta}{u_-\Lambda} = \left(\frac{2\pi^2 K_- g_\phi}{\Lambda^2 u_-}\right)^{\frac{1}{2-K_-/2}}. \quad \text{(D2)}$$

As Δ is affected by various parameters like u_-, K_-, and g_ϕ, once either of them develops randomness it must also fluctuate in space. We therefore replace $\Delta \mapsto \Delta + \delta\Delta(x)$, with $\langle\langle \delta\Delta(x)\delta\Delta(x')\rangle\rangle = D_\phi\delta(x-x')$.

Defining the dimensionless parameters $\mathcal{D}_\phi = \frac{\pi D_\phi}{u_-^2\Lambda}$, $\delta = \frac{\Delta}{u_-\Lambda}$ and performing an analysis along the lines described in Appendix B, the RG equations to leading order in $\mathcal{D}_\phi$ are given by

$$\frac{d\delta}{d\ell} = \delta\left(1 - \frac{8K_-\mathcal{D}_\phi}{1+\delta^2}\right)$$
$$\frac{d\mathcal{D}_\phi}{d\ell} = \mathcal{D}_\phi \quad \text{(D3)}$$

which can flow either to $(\delta = 0, \mathcal{D}_\phi = \infty)$ or to $(\delta = \infty, \mathcal{D}_\phi = \infty)$. The former is a disordered superconductor, with strong randomness in the gap—some kind of vortex glass, perhaps [42]; the exact nature cannot be determined from this approximate, perturbative approach. The latter case obeys $\frac{\mathcal{D}_\phi}{\delta} \to \text{Const.} < 1$, which means that the width of the distribution of δ gets smaller compared to δ itself.

This behavior exists, of course, in the bosonic insulator as well. However, it will never change the *structure* of the phase diagram, as it does not affect the fermionic intermediate sector. The superconducting phase, the intermediate disordered phase, and the intermediate ordered phase will all exist, and the main effect of this disorder in θ will be just inside the disordered insulating phase, where $\mathcal{D}_\eta$ is dominating anyway and drives the system to a disordered insulator state.

[1] For a review and extensive references, A. F. Hebard, in *Strongly Correlated Electronic Materials (The Los Alamos Symposium 1993)*, edited by K. S. Bedell, Z. Wang, D. E. Meltzer, A. V. Balatsky, and E. Abrahams (Addison Wesley, Boston, 1994), p. 251.

[2] S. L. Sondhi, S. M. Girvin, J. P. Carini, and D. Shahar, Rev. Mod. Phys. **69**, 315 (1997).

[3] A. M. Goldman and N. Markovic, Phys. Today **51**, 39 (1998).

[4] S. Sachdev, *Quantum Phase Transitions* (Cambridge University Press, Cambridge, England, 1999).

[5] M. P. A. Fisher, P. B. Weichman, G. Grinstein, and D. S. Fisher, Phys. Rev. B **40**, 546 (1989).

[6] T. Vojta, J. Crewse, M. Puschmann, D. Arovas, and Y. Kiselev, Phys. Rev. B **94**, 134501 (2016).

[7] M. P. A. Fisher and D. H. Lee, Phys. Rev. B **39**, 2756 (1989); M. P. A. Fisher, Phys. Rev. Lett. **65**, 923 (1990).

[8] M. P. A. Fisher, G. Grinstein, and S. M. Girvin, Phys. Rev. Lett. **64**, 587 (1990).

[9] E. S. Sø rensen, M. Wallin, S. M. Girvin, and A. P. Young, Phys. Rev. Lett. **69**, 828 (1992).

[10] M. C. Cha and S. M. Girvin, Phys. Rev. B **49**, 9794 (1994).

[11] N. Prokof'ev and B. Svistunov, Phys. Rev. Lett. **92**, 015703 (2004).

[12] E. Altman, Y. Kafri, A. Polkovnikov, and G. Refael, Phys. Rev. Lett. **93**, 150402 (2004); **100**, 170402 (2008); Phys. Rev. B **81**, 174528 (2010).

[13] P. Phillips, Science **302**, 243 (2003).

[14] A. Kapitulnik, S. A. Kivelson, and B. Spivak, Rev. Mod. Phys. **91**, 011002 (2019), and references therein.

[15] M. Mulligan and S. Raghu, Phys. Rev. B **93**, 205116 (2016).

[16] H. Goldman, M. Mulligan, S. Raghu, G. Torroba, and M. Zimet, Phys. Rev. B **96**, 245140 (2017).

[17] E. Orignac and T. Giamarchi, Phys. Rev. B **57**, 11713 (1998).

[18] A. Dhar, M. Maji, T. Mishra, R. V. Pai, S. Mukerjee, and A. Paramekanti, Phys. Rev. A **85**, 041602(R) (2012).

[19] A. Tokuno and A. Georges, New J. Phys. **16**, 073005 (2014).

[20] Z. Ristivojevic, A. Petkovic, P. Le Doussal and T. Giamarchi, Phys. Rev. B **90**, 125144 (2014).

[21] R. Shankar and G. Murthy, Phys. Rev. B **36**, 536 (1987); D. S. Fisher, Phys. Rev. Lett. **69**, 534 (1992); Phys. Rev. B **51**, 6411 (1995).

[22] Y. Atzmon and E. Shimshoni, Phys. Rev. B **83**, 220518(R) (2011).

[23] V. Mazo, C.-W. Huang, E. Shimshoni, S. T. Carr, and H. A. Fertig, Phys. Rev. B **89**, 121411(R) (2014); Phys. Scr. T **165**, 014019 (2015).
[24] J. M. Kosterlitz and D. J. Thouless, J. Phys. C: Solid State **6**, 1181 (1973)
[25] V. L. Berezinskii, Sov. Phys. JETP **34**, 610 (1972).
[26] A. Ghosal, M. Randeria, and N. Trivedi, Phys. Rev. B **65**, 014501 (2001); A. Datta, A. Banerjee, N. Trivedi, and A. Ghosal, arXiv:2101.00220.
[27] M. Sitte, A. Rosch, J. S. Meyer, K. A. Matveev, and M. Garst, Phys. Rev. Lett. **102**, 176404 (2009).
[28] L. Huijse, B. Bauer, and E. Berg, Phys. Rev. Lett. **114**, 090404 (2015).
[29] O. Alberton, J. Ruhman, E. Berg, and E. Altman, Phys. Rev. B **95**, 075132 (2017).
[30] T. Giamarchi, *Quantum Physics in One Dimension* (Oxford University Press, New York, 2004).
[31] P. Lecheminant, A. O. Gogolin, and A. A. Nersesyan, Nucl. Phys. B **639**, 502 (2002).
[32] A. O. Gogolin, A. A. Nersesyan, and A. M. Tsvelik, *Bosonization and Strongly Correlated Systems* (Cambridge University Press, Cambridge, England, 1998).
[33] T. Giamarchi and H. J. Schulz, Phys. Rev. B **37**, 325 (1988).
[34] M. Fabrizio, Phys. Rev. B **48**, 15838 (1993).
[35] O. Boada, A. Celi, J. I. Latorre, and M. Lewenstein, Phys. Rev. Lett. **108**, 133001 (2012).
[36] M. Mancini, G. Pagano, G. Cappellini, M. Livi, M. Rider, J. Catani, C. Sias, P. Zoller, M. Inguscio, M. Dalmonte, and L. Fallani, Science **349**, 1510 (2015); B. K. Stuhl, H. I. Lu, L. M. Aycock, D. Genkina, and I. B. Spielman, *ibid.* **349**, 1514 (2015).
[37] M. Calvanese Strinati, E. Cornfeld, D. Rossini, S. Barbarino, M. Dalmonte, R. Fazio, E. Sela, and L. Mazza, Phys. Rev. X **7**, 021033 (2017).
[38] Y. Cai, G. Zhang, and Y.-W. Zhang, J. Phys. Chem. C **119**, 13929 (2015).
[39] F. Hrahsheh and T. Vojta, Phys. Rev. Lett. **109**, 265303 (2012).
[40] J. Ruhman and E. Altman, Phys. Rev. B **96**, 085133 (2017).
[41] M. Calvanese Strinati, R. Berkovits and E. Shimshoni, Phys. Rev. B **100**, 245149 (2019).
[42] M. P. A. Fisher, Phys. Rev. Lett. **62**, 1415 (1989)